Deep Valley Radiation and Surface Energy Budget Microclimates. Part II: Energy Budget

C. DAVID WHITEMAN AND K. JERRY ALLWINE

Pacific Northwest Laboratory, Richland, Washington

LEO J. FRITSCHEN

University of Washington, Seattle, Washington

MONTIE M. ORGILL*

Pacific Northwest Laboratory, Richland, Washington

JAMES R. SIMPSON**

University of Washington, Seattle, Washington

(Manuscript received 25 March 1988, in final form 31 December 1988)

ABSTRACT

Surface energy budget measurements were made concurrently at five sites located on the valley floor, sidewalls and ridgetop of Colorado's 650-m deep Brush Creek Valley (39°32'N, 108°24'W) on the nearly clear day of 25 September 1984 using the Bowen ratio energy budget technique.

Daily average surface heat flux values for a natural sagebrush ecosystem on the floor of the semiarid valley included an input of 109 W m^{-2} net all-wave radiation and 15 W m^{-2} ground heat flux, and a loss of 48 W m^{-2} latent heat flux and 76 W m^{-2} sensible heat flux. Significant differences in instantaneous, daily, and daytime fluxes occurred from site to site as a function of slope aspect and inclination angles and surface properties, including vegetation cover and soil moisture.

Strong contrasts in instantaneous latent and sensible heat fluxes occurred between the opposing northeast- and southwest-facing sidewalls of the valley as solar insolation varied through the course of the day and as shadows propagated across the valley. This differential heating and moistening of the air above the opposing slopes produces cross valley circulations and the resulting moisture and heat transports observed by other investigators.

The ridgetop site, with a nearly unobstructed view of the sky and the longest daytime period, received the highest daily total of net radiation (12.12 MJ m^{-2}) and lost the highest sensible heat flux total (8.49 MJ m^{-2}). The dry southwest-facing slope produced a nearly equivalent daily total sensible heat flux, despite the later sunrise and earlier sunset at this site, because of the dry soil, lack of vegetation, and intense afternoon radiation on the sloping surface. One of the valley floor sites, located in a wheatgrass meadow, produced a daily total latent heat flux (7.37 MJ m^{-2}) over four times larger than the dry southwest-facing sidewall. Mean daytime Bowen ratios varied from 0.86 at the valley floor meadow site to 7.60 on the southwest-facing sidewall.

Daily total sensible heat fluxes in the valley were much larger than required to destroy typical nocturnal temperature inversions, and the excess is available on clear fall days to grow deep convective boundary layers over the region. Hodographs show clockwise turning of the winds above the northeast-facing sidewall during the course of the day, counterclockwise turning on the southwest-facing sidewall, and clockwise turning on the floor of the narrow valley as the cycle of down-slope, down-valley, up-slope and up-valley winds is executed. The times of reversal of the slope and valley wind systems at the individual energy budget sites were closely related to the time of sign reversal of sensible heat flux, within the time resolution of the sensible heat flux data.

1. Introduction

Few observations are available to show the range of energy budget microclimates in an area of complicated, deeply dissected terrain (Miller 1981; Oke 1978). These differences in microclimate, however, are of important ecological significance, affecting the distribution of plant and animal species and the timing of various types of biological activity. Hydrological and meteorological characteristics of the complex terrain area are also expected to depend strongly on energy budget microclimates.

As part of the U.S. Department of Energy's Atmospheric Studies in Complex Terrain (ASCOT) program, five surface energy budget stations were installed

* Current affiliation: White Sands Missile Range, Las Cruces, New Mexico.

** Current affiliation: University of Arizona, Tucson, Arizona.

Corresponding author address: Dr. C. David Whiteman, Battelle Pacific Northwest Laboratory, P.O. Box 999, Richland, WA 99352.

and operated in Colorado's deep Brush Creek Valley during September and October of 1984. The focus of the Brush Creek Valley experiments was on the meteorological behavior of the valley, investigating the evolving valley thermal structure and the structure of the locally developed wind systems. This paper reports on a subexperiment to investigate the surface energy budget microclimates in the valley. Data from this subexperiment were to be used as input to atmospheric numerical models and to analyses of the mass, momentum and heat budgets of the nocturnal valley atmosphere. The five sites in the valley were chosen to be representative of the major topographic surfaces in the valley (valley floor, sidewalls and mesa top) so that the data would be useful for these purposes.

The reader is referred to the accompanying paper by Whiteman et al. (1989) for information on the Brush Creek Valley, the locations of the measurement stations, the vegetation cover at individual sites, and other information on the experimental setup that are not repeated here. This paper begins with a discussion of the measurements and the equations used in processing the surface energy budget data. This is followed by a comparison of energy budget measurements made at the Brush Creek energy budget stations on the nearly clear day of 25 September. Finally, the observed wind systems are discussed in terms of the local energy balance measurements.

2. Bowen ratio energy budget method

Surface energy budget measurements in the Brush Creek Valley were made using the Bowen ratio energy budget (BREB) technique. This technique had been used in previous complex terrain experiments by other investigators (Rott 1979; Halbsguth et al. 1984; Schädler 1982) and had the advantage of requiring small amounts of equipment and measurements. Commercial electric power was unavailable in the Brush Creek Valley and, because of access difficulties in the rugged terrain, two of the five stations had to be transported to their sites by helicopter. Small, battery-operated, field-portable BREB stations had been recently developed by one of the authors (Fritschen). An accompanying paper by Fritschen and Simpson (1989) report on the design and performance of the BREB stations used in the Brush Creek experiments. These experiments produced opportunities to compare the BREB measurements with adjacent measurements at a valley floor site made with the eddy correlation technique. This comparison is reported in an accompanying article by Doran et al. (1989) for a nighttime period when measurements were coincident.

a. *Convective fluxes*

The energy balance of a homogeneous surface is given by the following equation:

$$Q^* + Q_G + Q_H + Q_E = 0, \tag{1}$$

where Q^* is the net all-wave radiation, Q_G is the ground heat flux, Q_H is the surface sensible heat flux and Q_E is the surface latent heat flux. In this equation, all fluxes toward the surface, whether from the ground or the atmosphere, are defined to be positive.

Using the flux-gradient approach, sensible and latent heat fluxes can be written as

$$Q_H = \rho c_p K_H \left(\frac{\Delta T}{\Delta z} + \Gamma \right) \quad \text{and} \tag{2}$$

$$Q_E = -\frac{\epsilon \rho L_v}{P} K_W \frac{\Delta e}{\Delta z}, \tag{3}$$

where ρ is air density, c_p is specific heat of air at constant pressure, T is temperature, Γ is 0.0098° Cm^{-1}, z is height, ϵ is 0.622, L_v is latent heat of vaporization of water, P is atmospheric pressure, K_H and K_W are the eddy diffusivities for heat and water vapor, and e is vapor pressure.

The ratio β of the sensible and latent heat fluxes, termed the Bowen ratio, is then given by

$$\beta = \frac{Q_H}{Q_E} = \frac{\alpha c_p P}{\epsilon L_v} \left(\frac{\Delta T + \Gamma \Delta z}{\Delta e} \right). \tag{4}$$

The value of the ratio of the eddy diffusivities α is somewhat controversial, but is assumed here to be unity in accordance with assumptions made by others using the BREB method, and in the absence of definitive evidence for an alternative value. This is equivalent to assuming that turbulence is equally effective in transporting thermal energy and water vapor.

In the BREB method, net all-wave radiation and ground heat flux are measured along with gradients of air temperature and vapor pressure over a given height interval. The convective fluxes are then calculated as

$$Q_E = -\frac{1}{1+\beta}(Q^* + Q_G) \quad \text{and} \tag{5}$$

$$Q_H = \beta Q_E. \tag{6}$$

In such calculations, one assumes that the sensible and latent heat fluxes do not change over the height of the gradient measurements and that the measurements are averaged over an interval long enough to get an adequate statistical sample but short enough that the atmosphere is nearly steady state. A 30-min averaging period was chosen to satisfy this latter requirement. The heights of the gradient measurements for the Brush Creek stations are given in Table 1. These heights were chosen based on the surface cover at the individual sites. Further information on the experimental sites is given in the accompanying article by Whiteman et al. (1989).

Sites were chosen to minimize the effects on the surface energy budget measurements of sharp upwind discontinuities in surface cover or topography. Uniformity of the fetch, however, was difficult to evaluate in practice. Shallow benches were present below both sidewall sites, although they produced no sharp changes in veg-

TABLE 1. Instrument heights.

Site	Instrument height (m)	
	Anemometer	Psychrometer
PNL	2.48	1.17–2.17
RDG	2.48	0.79–1.76
E	2.37	0.60–1.77
W	2.18	1.27–2.27
WPL	2.48	0.51–1.57

etation or, apparently, moisture. The meadow site, on the other hand, was significantly more moist than the natural mountain shrub and desert sagebrush ecosystems on the nearby sidewalls and was probably somewhat more moist than adjacent areas on the valley floor. The effects of surface cover, topography, and moisture discontinuities on the measurement of fluxes have not been investigated in the present experiments, and this is an important question that should receive additional research in future studies.

b. *Net radiation and ground heat flux*

Determination of sensible and latent heat fluxes from (5) and (6) requires knowledge of the Bowen ratio β, obtained from measurement of vertical gradients of temperature and vapor pressure using (4), and accurate measurement of net radiation and ground heat flux.

Net all-wave radiation measurements were made with identical miniature net radiometers calibrated by the manufacturer before the experiment. Measurements made on horizontal radiometers at the two sidewall sites were translated to the underlying sloping surfaces using the method described by Whiteman et al. (1989). Values of all four surface energy budget components at all sites (three horizontal sites and two sidewall sites) are reported per square meter of the underlying surface.

Ground heat fluxes were measured perpendicular to the local ground surface, so that measured soil heat fluxes at the sidewalls sites are expected to be representative of the ground heat flux per square meter of sloping surface. Determination of the ground heat flux at the surface (Q_G) involves the measurement of the soil heat flux at some depth (Q_F) plus the calculation of the change in energy storage in the layer of soil above the heat flux transducer (Q_S), such that

$$Q_G = Q_F + Q_S. \tag{7}$$

Soil heat flux density was measured at all sites with Micromet Instruments heat flow transducers at 0.1 m depth. Since thermal conductivity of a transducer is generally different from that of the soil, measured soil heat fluxes Q'_F were corrected to obtain actual soil heat flux using the formula

$$Q_F = Q'_F \frac{1 - 1.92\frac{l}{d}\left(1 - \frac{\lambda_G}{\lambda_T}\right)}{1 - 1.92\frac{l}{d}\left(1 - \frac{\lambda_M}{\lambda_T}\right)}. \tag{8}$$

This correction (Fritschen and Gay 1979) is based on the theory developed by Philip (1961) in which the ratio of the heat flow through the transducer to the heat flow through the soil is related to the transducer thermal conductivity λ_T, soil thermal conductivity λ_G, and the thermal conductivity of the calibration medium λ_M, where l and d are the thickness and diameter of the cylindrical transducer. The thermal conductivity of the transducer and calibration medium were determined in the laboratory before the field experiment and the thermal conductivity of the soil was determined from a formula for silt loam soils determined by McInnes (1981), as presented by Campbell (1985):

$$\lambda_G = A + B\chi_W - (A - D)\exp[-(C\chi_W)^4], \tag{9}$$

where χ_W is the volume fraction of water in the soil and the coefficients are a function of soil bulk density ρ_B and soil clay fraction χ_C:

$$\begin{aligned} A &= 0.65 - 0.78\rho_B + 0.60\rho_B^2 \\ B &= 1.06\rho_B \\ C &= 1 + 2.6\chi_C^{-0.5} \\ D &= 0.03 + 0.1\rho_B^2. \end{aligned} \tag{10}$$

Bulk soil densities and soil clay, mineral and organic fractions were estimated (Table 2) using a Soil Conservation Service soils map of the Brush Creek Valley and published laboratory analyses of soil samples taken from the adjacent Clear Creek Valley (Moore et al. 1981). Soil samples were collected at each of the measurement sites during the course of the experiments to allow the post-experiment laboratory determination of soil moisture by standard gravimetric procedures (ASTM-D2216-80).

Change in heat storage in the soil above the heat flux plate was determined using the formula

$$Q_S = -C\frac{\Delta T_S}{\Delta t}\Delta Z_S, \tag{11}$$

where C is the volumetric soil heat capacity, T_S is the

TABLE 2. Soil coefficients.

	ρ_B (10^3 kg m^{-3})	χ_c —	χ_0 —	χ_M —	χ_W —
PNL	1.2	0.07	0.04	0.46	0.075
RDG	1.3	0.13	0.05	0.45	0.110
E	1.4	0.07	0.02	0.48	0.050
W	1.3	0.09	0.07	0.43	0.185
WPL	1.2	0.08	0.10	0.40	0.175

mean soil temperature in the layer from 0 to 0.1 m and ΔZ_S is 0.1 m. Mean soil temperature was measured with four equally spaced silicon diodes wired in parallel and potted in epoxy in the form of a 0.1 m long rod.

Data collection system resolution of the measured mean soil temperatures was 0.14°C. This was, unfortunately, too coarse, and produced steps in the soil temperature curves rather than the desired smooth curves. A five-point running mean was consequently applied to the mean soil temperature data to reduce the problem.

Soil samples were used to estimate the volume fractions of soil constituents to calculate the soil heat capacity using the formula

$$C = C_M\chi_M + C_0\chi_0 + C_W\chi_W + C_A\chi_A, \quad (12)$$

where subscripts on volumetric heat capacity C and volume fraction χ refer to minerals, organic matter, water and air, respectively, and

$$\chi_A = 1 - \chi_M - \chi_0 - \chi_W. \quad (13)$$

Volumetric heat capacities of $C_W = 4.2$, $C_0 = 2.5$ and $C_a = 0.001$ MJ m^{-3} K^{-1} were obtained from published tables (e.g., Campbell 1985). The volumetric heat capacity of the mineral fraction of the Brush Creek soils, $C_M = 1.3$ MJ m^{-3} K^{-1}, was derived from laboratory specific heat measurements of oven-dried soil samples, obtained after grinding.

3. Processing of data

a. Bowen ratio data

Psychrometric data at the Bowen ratio stations were obtained at two levels using identical shielded fan-aspirated updraft psychrometers (see Table 1 for heights). The resolution of the temperature and wet bulb temperature sensors was nominally 0.006°C. To reduce experimental error in the measured temperature and humidity gradients, the psychrometers were interchanged with a belt-driven Automatic Exchange Mechanism (AEM) every 6 min. Further details on the equipment and its performance are provided by Fritschen and Simpson (1989).

All basic radiation and surface energy budget data were sampled at 30-s intervals for the last 4 out of every 6 min. At the conclusion of each 6-min sampling period the AEM was activated, and sampling of all data was stopped for a 2-min period while the psychrometers equilibrated at their new levels. The basic data set thus consists of 4-min average data at 6-min intervals corresponding to the time periods during which the psychrometers maintained their positions. A moving 12-min average was applied to the resulting dataset to account for the psychrometer interchanges, and 30-min average surface energy budget quantities were, in turn, obtained from five overlapping 12-min averaged data points. The ending time (LST) was assigned to each 30-min averaged value.

b. Alternate method of calculating fluxes

The data processing objective was to use the BREB data to the maximum extent. The BREB method of calculating convective fluxes fails, however, when the Bowen ratio approaches −1 [see Eq. (5)]. This typically occurs twice per day during a brief transition period in the morning and afternoon. Further, during nighttime or in other low flux situations when inaccuracies in measurements of net radiation and ground heat flux are comparable to the convective fluxes, erroneous results may be obtained. This is apparent in the data when the calculated fluxes are inconsistent with the sign of the measured gradients. We used Ohmura's (1982) objective method to reject erroneous BREB data, but modified his method slightly to reject all calculated fluxes for which the Bowen ratio was between −0.75 and −1.25.

An alternate method of calculating convective fluxes was developed for periods when the objective criteria required rejection of the BREB fluxes or when the vapor gradient data were incomplete or untrustworthy (e.g., frozen or dry wicks). In these cases, a combined energy budget-aerodynamic method suggested by Tanner (1967) was used to fill in the missing data periods. This method uses the bulk aerodynamic method to determine an exchange coefficient

$$C_v = \epsilon Q_H / c_p P u \Delta T, \quad (14)$$

where u is the wind speed. Following Deardorff (1968), we assumed that C_v at each site is solely a function of the bulk Richardson number,

$$R_B = \frac{g}{T}\frac{\Delta\theta}{\Delta z}\left(\frac{z_u}{u}\right)^2, \quad (15)$$

where g is gravitational acceleration, θ is potential temperature, and z_u is the height at which wind speed u is measured.

The procedure is to use all nonrejected Bowen ratio data to develop a relationship between C_v and R_B using (14) and (15). Then, for periods when Bowen ratio data are rejected, R_B is calculated from the wind and temperature profile data using (15), and C_v is determined from the relationship between R_B and C_v. The value of C_v is then entered into (14) to calculate a 6-min average Q_H. The C_v–R_B relationships were developed for each station (Table 3) using data collected during a 16-day period. Figure 1 illustrates the C_v–R_B relationship for the PNL station. Fritschen and Simpson (1989) presented a similar relationship for wheat stubble in Kansas.

For 30-min periods when some 6-min average Bowen ratio data were rejected, the aerodynamic method was used to substitute for the rejected 6-min Bowen ratio sensible heat flux data; the 30-min average latent heat flux was then calculated as an energy balance residual so that an energy balance is always maintained.

For periods when data were missing, 30-min net ra-

TABLE 3. Exchange coefficient–bulk Richardson number relationships.

Site	Relationship	Condition
PNL	$C_V = -13.300R_B + 0.436$,	$R_B < 0.020$
	$C_V = -0.389R_B + 0.178$,	$R_B \geq 0.020$
RDG	$C_V = -15.679R_B + 0.402$,	$R_B < 0.011$
	$C_V = 0.000R_B + 0.230$,	$R_B \geq 0.011$
E	$C_V = -10.000R_B + 0.250$,	$R_B < 0.000$
	$C_V = 0.000R_B + 0.250$,	$R_B \geq 0.000$
W	$C_V = -18.209R_B + 0.772$,	$R_B < 0.027$
	$C_V = -0.867R_B + 0.303$,	$R_B \geq 0.027$
WPL	$C_V = -7.480R_B + 0.350$,	$R_B < 0.027$
	$C_V = 0.000R_B + 0.150$,	$R_B \geq 0.027$

diation, ground heat flux and sensible heat flux data were interpolated, with latent heat flux calculated as a residual. We found that it was occasionally necessary to subjectively edit 6-min data when there was a significant mismatch between BREB data and inserted aerodynamic values.

4. Surface energy balance

Data will be presented for 25 September 1984—a nearly clear day, although a few cirrus clouds were present in the early morning hours, and a layer of cirrostratus made several advances into the valley from the south in the mid- to late afternoon. The first freezing temperatures of the field study, and presumably the season, in the Brush Creek Valley occurred on this morning at all sites.

Figure 2 shows the diurnal variation of net radiation, ground heat flux, latent heat flux, and sensible heat flux at the five sites obtained with the methods described above. Table 4 presents the daily and daytime (local sunrise to local sunset, i.e., LSR–LSS) surface energy budget component totals obtained by integration of the curves in Fig. 2. Also included in Table 4

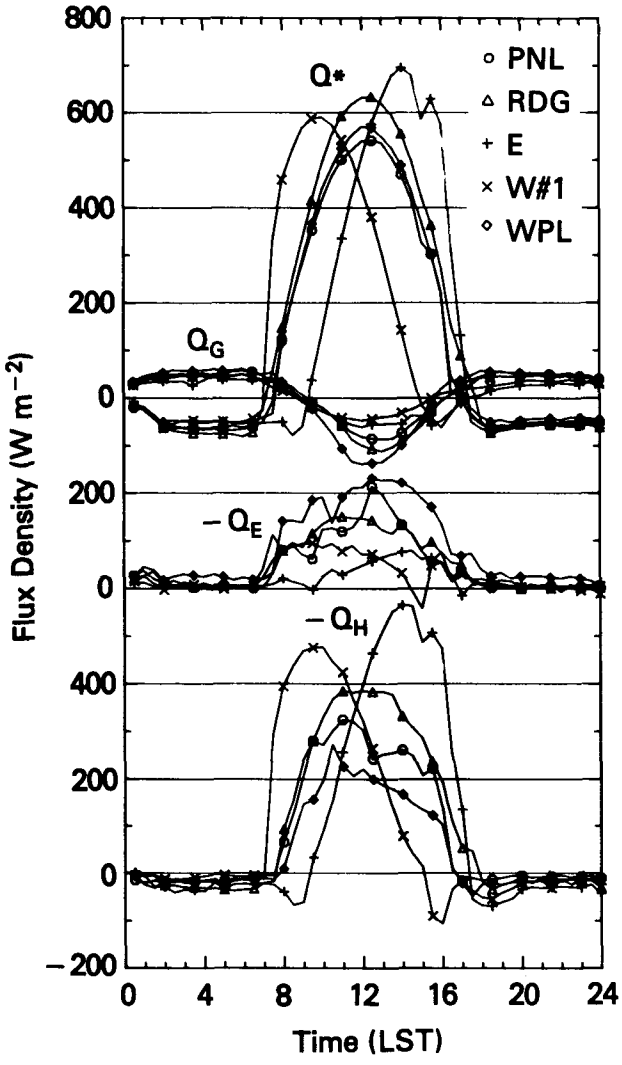

FIG. 2. Net all-wave radiation flux (Q^*), soil heat flux (Q_G), latent heat flux (Q_E) and sensible heat flux (Q_H) for five sites in the Brush Creek Valley, 25 September 1984.

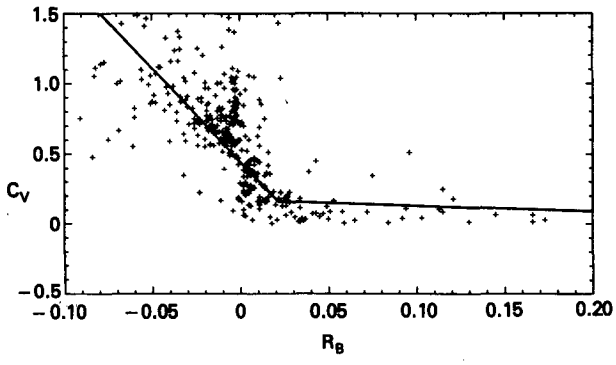

FIG. 1. Exchange coefficient versus Richardson number for the PNL valley floor site, using 30-min averaged data from the period 16 September through 1 October 1984.

are several diagnostic ratios of the various energy budget totals. The difference (not shown) between the daily and daytime totals would represent the nighttime (LSS–LSR) totals. Plots of daily and daytime heat flux totals for all sites are presented in Fig. 3a and b, respectively.

At the lower valley floor (PNL), ridgetop (RDG), and upper valley floor or meadow (WPL) sites, located on level ground, net radiation (Fig. 2) was symmetric about solar noon, with the highest 30-min average net radiative gain at the ridgetop site (634 W m^{-2} at 1230 LST). Strong asymmetries occurred at the east (E) and west (W) sidewall sites because the slope and aspect angles of the sidewalls strongly affect the timing and magnitude of the radiation income. The largest 30-min average net radiative gain of all the sites (695 W

TABLE 4. Surface energy balance totals (MJ m^{-2}) for 25 September 1984 calculated from 30-min averages, and ratios of the various totals.

Site	Times	Q^*	Q_G	Q_H	Q_E	Q_H/Q^*	Q_G/Q^*	Q_H/Q_E	$Q_E/(Q^* + Q_G)$
				Daily totals					
PNL	0000–2400	9.45	1.32	−6.60	−4.17	−0.70	0.14	1.58	−0.39
RDG	0000–2400	12.12	0.75	−8.49	−4.38	−0.70	0.06	1.94	−0.34
E	0000–2400	9.74	0.47	−8.43	−1.77	−0.87	0.05	4.76	−0.17
W	0000–2400	8.52	1.40	−7.43	−2.49	−0.87	0.16	2.98	−0.25
WPL	0000–2400	10.45	0.94	−4.04	−7.37	−0.39	0.09	0.55	−0.65
				LSR–LSS* totals					
PNL	0730–1630	12.14	−1.29	−7.21	−3.65	−0.59	−0.11	1.98	−0.34
RDG	0630–1800	14.76	−1.20	−9.44	−4.11	−0.64	−0.08	2.30	−0.30
E	0830–1700	12.67	−1.15	−10.18	−1.34	−0.80	−0.09	7.60	−0.12
W	0700–1500	11.14	−0.68	−8.60	−1.86	−0.77	−0.06	4.62	−0.18
WPL	0800–1630	12.71	−1.88	−5.00	−5.84	−0.39	−0.15	0.86	−0.54

* LSR–LSS = local sunrise to local sunset.

m^{-2} at 1400 LST) was experienced at the east sidewall site. Nighttime net radiative losses at the five sites, except for a cloudy period after midnight, were typically 50–65 W m^{-2}. As an example of the differences between sites, at 0500 LST net radiative losses were 67, 76, 62, 49, and 50 W m^{-2} at the PNL, ridgetop, east sidewall, west sidewall and meadow sites, respectively. The highest losses occur at the ridgetop site where the sky view factor (sky fraction of the upper hemisphere) was large (0.92). Other factors at individual sites that appear to affect nighttime radiative fluxes were the surface cover (e.g., grasses at the WPL site become radiatively cold during nighttime) and the existence of a nighttime temperature inversion in the valley, which increases the atmospheric radiation received at the slope sites relative to the other sites. Unusual dips in the nighttime net radiation curves (Fig. 2) for the east sidewall site near sunrise and for the west sidewall site near sunset are artifacts of the method used to translate horizontal net radiation measurements at these two sites to the underlying sloping surfaces.

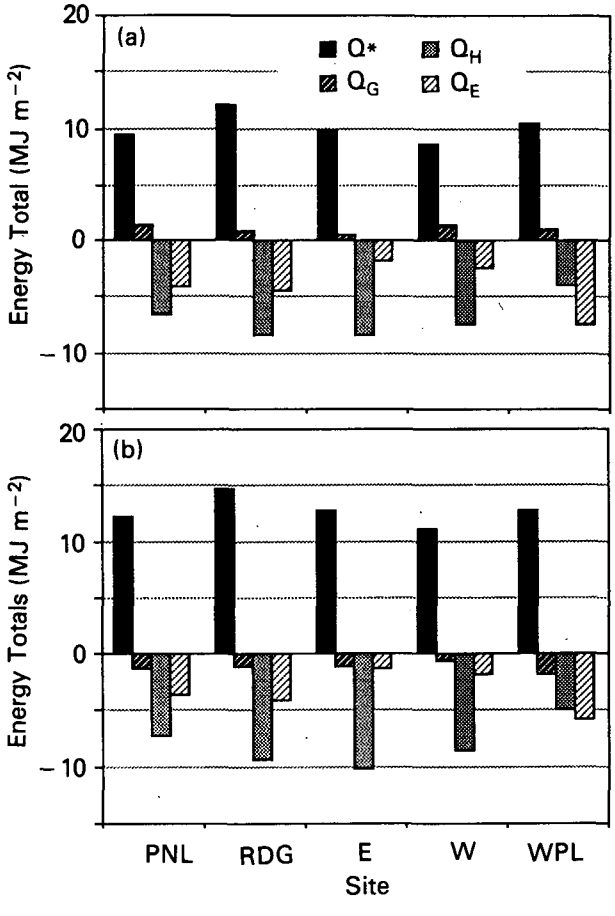

FIG. 3. (a) Daily and (b) daytime (i.e., local sunrise time to local sunset time) heat flux totals at the five Brush Creek Valley sites, 25 September 1984.

Net radiation totals at all sites except for the ridgetop site are significantly affected by the delayed sunrise and early sunset caused by topographic shading from the surrounding ridgetops. This effect is quite pronounced at the west sidewall site, where local sunset occurs in early afternoon. Daytime totals of net all-wave radiation were highest at the ridgetop site (14.76 MJ m^{-2}), which had the longest period of direct sunlight (11.5 h), and lowest at the west sidewall site (11.14 MJ m^{-2}), which had the shortest period of direct sunlight (8 h). The east sidewall site had an intermediate value of net all-wave radiation (12.67 MJ m^{-2}), despite its short daytime period (8.5 h), on account of the high net radiation values received during early to midafternoon when the southwest-facing slope faces the sun directly. This effect of the slope's orientation would have been greater still, had it not been for midafternoon cirrostratus clouds.

Heat flux into the ground (Fig. 2) typically began an hour or more after local sunrise at all sites and ended before local sunset. The largest daytime ground heat

flux (-139 W m^{-2}) occurred at the moist meadow site while the smallest (-53 W m^{-2}) occurred at the west sidewall site. Nighttime ground heat fluxes at the five sites were directed toward the surface at rates of up to 50–60 W m^{-2}. These ground heat fluxes effectively balanced much of the nighttime net radiative energy loss from the surfaces, with the result that little available energy ($Q^* + Q_G$) was left for sensible and latent heat fluxes. The amplitude of the ground heat flux curves was highest at the meadow and ridgetop sites. The dry east sidewall site had the lowest nighttime ground heat flux and one of the lowest daytime fluxes. During daytime, heat flux into the ground at the west sidewall site was low despite the relatively moist soils that supported the growth of a dense cover of bushes on this sidewall. At this sidewall the highest net radiative fluxes occurred in the morning hours and the energy was initially used to evaporate water and heat the air. The bushes shaded the ground effectively when shadows were long in the morning, and the cover of organic debris reduced ground heat fluxes. The daytime ground heat flux curve was thus strongly damped while the nighttime curve appeared to differ little from the other sites. Thus, over the course of this fall day the daily soil energy loss was highest on the west sidewall.

Daytime ground heat flux totals at the five sites were in the range from -0.68 to -1.88 MJ m^{-2}, but a long nighttime period of modest energy loss at the rate of 40 or 50 W m^{-2} produced a net loss of energy from the soil on this clear fall day, thereby producing seasonal cooling of the ground as winter approached. Daytime ground heat flux totals were 0.06–0.15 of the daytime net all-wave radiation totals, but nighttime ground heat fluxes constituted over 0.50 of the nighttime net radiation totals at all sites. The near-equivalence of nighttime ground heat flux and net all-wave radiative loss made the measurement of sensible and latent heat fluxes by the BREB method difficult at night and increased uncertainty in the nighttime results.

Evaporation continued day and night at all sites. Latent heat flux magnitudes, however, were relatively small compared to observations in wetter climates (e.g., Oke 1978). The western wheatgrass meadow at the meadow site produced the highest instantaneous latent heat flux (-232 W m^{-2}), while latent heat flux at the dry east sidewall site attained only -79 W m^{-2}. Latent heat flux at the ridgetop site was nearly symmetric about solar noon, but the PNL and meadow sites exhibited somewhat higher fluxes in the afternoon. Latent heat fluxes were high on the west sidewall in the morning and on the east sidewall in the afternoon, in keeping with the asymmetric course of net radiation at the two sites.

Daily latent heat flux totals differed at the five sites, depending on vegetation and soil moisture. The east sidewall site was on a barren slope containing little vegetation and very dry soil (Table 2). Daily total latent heat flux at this site was -1.77 MJ m^{-2}, equivalent to the evaporation of 0.7 mm of water. The meadow site, although not irrigated, was in a moist valley floor setting. Evapotranspiration at this site produced a daily total latent heat flux of -7.37 MJ m^{-2}, equivalent to the loss of 3.0 mm of water. These levels of latent heat flux represent 0.17–0.65 of the daily available energy at the two sites.

Sensible heat fluxes differed significantly from site to site, with especially pronounced differences between the east and west sidewalls. Fluxes were a maximum on the west sidewall in the morning (-477 W m^{-2} at 1000 LST) and on the east sidewall in the afternoon (-565 W m^{-2} at 1400 LST). Daytime fluxes over the sidewalls heated the near-surface layer of air creating buoyancy forces that drove upslope winds. These flows will be discussed in a later section of this paper. Only at 1130 LST were daytime sensible heat fluxes equivalent over the two sidewalls. Before 1130 sensible heat fluxes were larger over the west sidewall and after 1130 they were higher over the east sidewall. Differential atmospheric heating rates above the opposing sidewalls drive a cross-valley flow toward the more strongly heated sidewall. The effect of the morning cross-valley flow on the dispersion of an elevated tracer plume in the Brush Creek Valley has been studied previously by Whiteman (1989) and, with a two-dimensional numerical model, by Bader and Whiteman (1989). On the valley floor sensible heat flux was higher in the morning than in the afternoon. This seems to have been caused by two factors. Since the ground heat flux wave lags the net radiation, the morning input of net radiation is channeled into the two convective fluxes, with little energy lost to the ground. This tends to increase the convective fluxes in the morning relative to the afternoon. Also, there seems to be a relatively larger flow of this available energy into sensible heat flux than into latent heat flux in the morning. Partitioning of much of the available energy into latent heat flux at the meadow site reduced the sensible heat flux there. At the ridgetop site, the sensible heat flux curve was symmetrical about solar noon. The maximum value (-385 W m^{-2}) was less than that at the dry east sidewall site, where sensible heat flux attained -565 W m^{-2} in the afternoon when the sun was shining directly on the inclined surface and there was little transpiration from the sparse vegetation and thermal diffusivity of the dry soil was low. The topmost soil layer became strongly heated; measurements of upward longwave radiation from the site showed effective radiating temperatures (ϵ assumed equal to 1) as high as 30.5°C, nearly 9°C higher than the WPL and ridgetop sites.

Nighttime values of sensible heat flux were generally in the range from 5 to 40 W m^{-2}, except for a 3-h period of higher fluxes (nearly 70 W m^{-2}) in the early evening. Confidence in the nighttime convective fluxes is relatively low. Some nighttime Bowen ratio calculations were rejected using the Ohmura (1982) test, and additional difficulties were experienced with some

of the automatic exchange mechanisms and with frozen psychrometers.

Daytime totals of sensible heat flux varied from -5.00 MJ m^{-2} at the meadow site, where much of the available energy was used to support evapotranspiration, to -10.18 MJ m^{-2} at the east sidewall site. The daytime sensible heat flux total at the ridgetop site (-9.44 MJ m^{-2}) rivaled the total at the east sidewall site. This was primarily due to the increased length of the daytime period at the ridgetop site, even though 30-min average fluxes never rose above -385 W m^{-2} in magnitude. Nighttime sensible heat fluxes were also largest in magnitude at the ridgetop site. These observations lend support to the concept of the valley ridgetops being elevated sources of warm air during the day and cold air during the night, supporting the development of along-slope and mountain–plain wind circulations.

The distribution of available energy between the two convective fluxes is a key climatological characteristic of a given site. This distribution has traditionally been specified by the Bowen ratio, the ratio of sensible to latent heat flux. Bowen ratios (Table 4) range from 0.86 at the meadow site to 7.60 at the east sidewall site. Alternative measures of this distribution are the ratios of latent heat flux and sensible heat flux to available energy. These ratios are fractions whose absolute values sum to one. From Table 4 we see that 0.12 of the available energy is converted to latent heat at the east sidewall site during daytime and 0.54 is converted to latent heat at the meadow site.

It is interesting to compare the daytime sensible heat flux totals to the energy required to destroy nocturnal valley temperature inversions. This energy requirement can be calculated from near-sunrise valley temperature sounding data using the first law of thermodynamics. For a vertical cross section of the valley at a location where the valley is 4.3 km wide (ridgetop to ridgetop), the energy requirement per meter in the along-valley direction, using typical sunrise temperature soundings, is about 5000 MJ m^{-1}. This is equivalent to a mean flux of 1.2 MJ m^{-2} out the area at the top of the valley cross section. When this number is compared to the daytime total sensible heat flux at a typical location, say the PNL site at 7.21 MJ m^{-2}, it is clear that sensible heat fluxes on representative clear days in the fall are more than sufficient to destroy the nocturnal temperature inversions. The excess energy is available to develop deep convective boundary layers (CBLs) above the western slope of the Colorado Rocky Mountains (Laulainen et al. 1981). The effect of CBLs on valley ecosystems is significant. The large excess of energy is responsible for regular diurnal changes in valley thermal stratification. Convective boundary layer growth mixes pollutants and moisture trapped in the valley circulations at night through a deep layer of the atmosphere during the day and couples the valley wind systems to the flows above the valley.

5. Valley wind structure evolution and its relationship to the energy balance

Figure 4 provides a schematic diagram of the diurnal course of the wind systems on the opposite sidewalls of an idealized, arbitrarily oriented, valley. On the river's right bank (i.e., the left sidewall of the valley in Fig. 4), the winds turn in a clockwise direction, while on the river's left bank the winds turn counterclockwise with time. Sequenced in time, sidewall winds turn from down-valley, to upslope, to up-valley, to downslope, although in actual situations it is often difficult to find pure along-slope or along-valley winds, as these winds systems interact closely (Hennemuth and Schmidt 1985).

Hodographs of one-hour mean vector winds observed by anemometers at the five BREB sites (see Table 1 for anemometer heights) are presented in Fig. 5. Hodographs at the ridgetop site show no looping indicative of slope-valley wind interactions, but are indicative of the above-valley winds prevailing at ridgetop level. These were from the northeast in the first half of the day, shifting nearly 180 degrees to southwest between 1000 and 1200 LST.

Winds turn clockwise at the west sidewall site (i.e., Brush Creek's right bank) and counterclockwise at the east sidewall site, as expected. Perhaps the most interesting features of the hodographs are the times of windshifts and their relationship to the local times of sunrise and sunset and the change of sign of sensible heat flux on the individual slopes. For example, at the west sidewall site, early morning winds are initially down-slope and down-valley. Winds shift to upslope around 0700 LST as the slope is illuminated by the sun and sensible heat flux becomes positive. Winds maintain their upslope component but shift to up-valley about an hour later. Local sunset occurs at 1430 LST at the west sidewall site. At this time the local

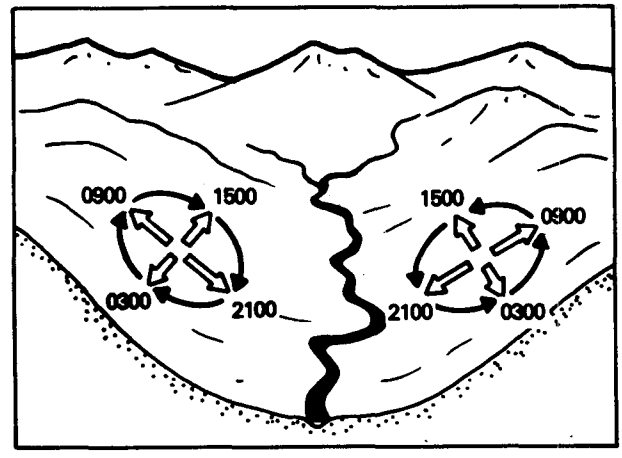

FIG. 4. Turning of the winds with time on the opposite sidewalls of an idealized valley (after Hawkes 1947).

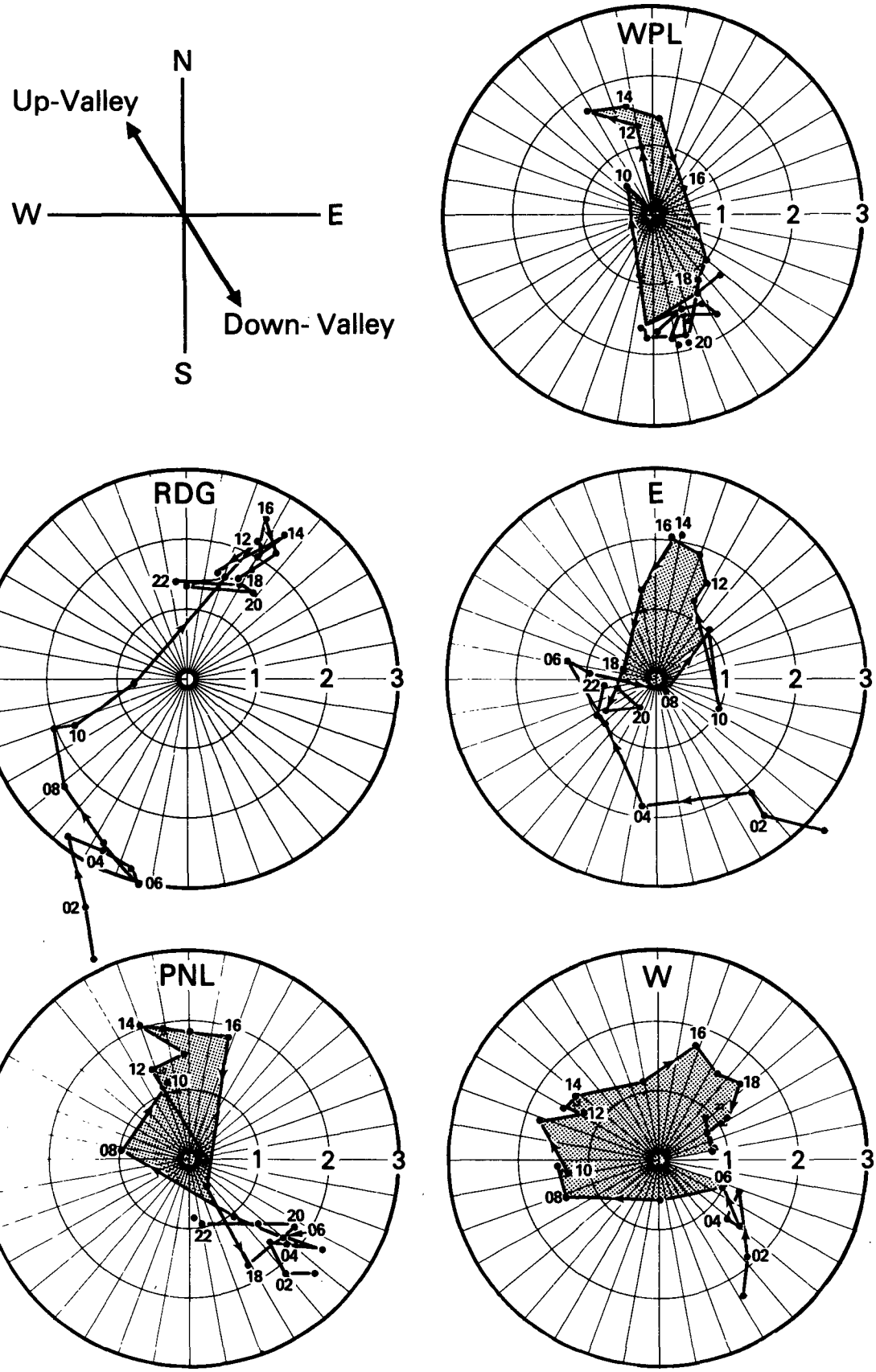

FIG. 5. Hodographs from wind data collected at the five BREB stations, 25 September 1984. Indicated times (LST) are the midpoints of 1-h-averaged vector winds. Windspeeds in m s^{-1}.

energy balance at the slope reverses, and downward sensible heat flux begins to cool a layer of air just above the slope. The upslope wind quickly reverses to downslope, but the up-valley wind, responding to the energy budget of the valley as a whole rather than to the local energy budget over the slope, continues to blow for many hours. In fact, one sees that the down-valley flow is not well-marked at the altitudes of either of the slope sites on this evening, although well-marked on the valley floor. One feature of the meteorology of the Brush Creek Valley is the ready drainage of cold air from the valley at night in a shallow layer just above the valley floor (Whiteman and Barr 1986; Post and Neff 1986). On the evening of 25 September and morning of 26 September, winds above this shallow layer actually blew up-valley in apparent response to an up-valley component of synoptic winds above the valley (Gudiksen and Shearer 1989).

Winds on the east sidewall also follow the pattern of sensible heat flux influence discussed above for the west sidewall. Winds before 0400 LST are anomalous, presumably caused by an episode of high clouds (see Fig. 2) that reduced downward sensible heat flux over the entire valley. After 0400 LST, the nighttime down-valley and downslope flow persisted until upslope flow was initiated between 0800 and 0900 LST. Persistent up-valley winds began on this slope only between 1000 and 1100 LST. Downslope flow began near sunset (after 1700 LST).

The valley floor stations show a clear signature of the slope-valley wind interactions, although up- and down-valley winds are predominant at these sites. Winds at the valley floor sites turn clockwise in response to the change with time of the fluxes of sensible heat over the adjacent sidewalls. The strong illumination of the dry, east sidewall in the afternoon produces large sensible heat fluxes that drive marked cross-valley winds at the valley floor sites.

6. Summary and conclusions

The Bowen ratio energy budget technique has been used to measure components of the surface energy budget at five sites in Colorado's semiarid Brush Creek Valley on the nearly clear day of 25 September 1984. Individual short- and long-wave components of the radiation balance were described in the accompanying paper by Whiteman et al. (1989).

A natural sagebrush ecosystem on the valley floor (PNL site) may be used to illustrate typical surface energy budget components in the semiarid Brush Creek Valley for clear days near the time of the autumnal equinox. The radiation balance of the surface is characterized by an excess of shortwave radiation gain relative to the 24-h longwave loss, in the amount of 109 W m^{-2}. The surface receives a 24-h average net heat flux from the soil in the amount of 15 W m^{-2}. This net available energy at the surface (109 + 15 = 124 W m^{-2}) is used to evaporate water (48 W m^{-2}) and to heat the air above the surface (76 W m^{-2}).

This study focuses on the differences in valley energy budget components measured concurrently at multiple sites in an area of complex deep valley topography. The study shows that significant differences between sites occur in all components of the energy budget. Net all-wave radiation differs significantly in timing and in magnitude on the opposing sidewalls as a function of slope aspect and inclination angles. Daytime and nighttime net radiation totals were highest on the ridgetop plateau, supporting the concept of the elevated plateaus being elevated sources of heat in daytime and cooling during nighttime.

Ground heat fluxes varied from site to site depending mostly on soil moisture and vegetation cover. Ground heat flux totals during daytime were typically 0.06–0.15 of the net radiation flux totals. During nighttime, however, the upward flux of heat from the soil balanced much of the net all-wave radiative loss.

Observations in the valley showed that evaporation continued day and night. Daytime latent heat flux totals at the five sites varied over a factor of 4.4. Largest daytime evaporation occurred at a meadow site on the valley floor, where latent heat fluxes utilized 0.54 of the available energy. The natural ecosystems in the valley (including a nearly barren sidewall, a sagebrush ecosystem, and a mountain shrub ecosystem) showed much lower evaporation; during daytime, latent heat fluxes from these ecosystems used 0.12 to 0.34 of the available energy.

Sensible heat flux totals differed by as much as a factor of two at the five sites. The high levels of sensible heat flux during daytime are easily sufficient to destroy typical nighttime temperature inversions. The excess energy, once the inversions are destroyed, can provide the energy necessary to grow the deep convective boundary layers observed by other investigators over the western Colorado region.

Observations show that latent and sensible heat fluxes differ strongly on the opposite sidewalls of the valley as a function of time of day. The consequence is to create different rates of heating and moistening of the atmosphere over the two slopes and should have the effect of creating horizontal temperature and humidity gradients. This would lead to cross valley circulations which blow towards the more strongly heated slope and act to distribute heat and moisture through the valley cross section.

Locally developed wind systems were strongly forced by the time-varying sensible heat flux field in the valley. Solar shading from the surrounding ridges played an important role in the energy balances at the individual sites in this deep valley, and strongly affected the daily surface energy balance totals.

Work is currently under way to use a digital topographic model and the Brush Creek Valley surface energy budget measurements to estimate components of

the radiation and surface energy budgets over the entire watershed. Work is also continuing to evaluate the components of the surface energy balance on other experimental days. This information will be used to investigate the energy budget of the valley atmosphere during nighttime, following an initial approach outlined by Horst et al. (1987). The sensible heat flux calculations will also be used to support atmospheric modeling of the local circulations that develop in the valley.

Acknowledgments. The research was supported by the U.S. Department of Energy under Contract DE-AC06-76RLO 1830 with Pacific Northwest Laboratory. Pacific Northwest Laboratory is operated by Battelle Memorial Institute for the U.S. Department of Energy. Mr. Dave Alstatt of the Soil Conservation Service and Mr. T. Bargsten of the Bureau of Land Management in Grand Junction, Colorado, are thanked for their help in estimating physical properties of the Brush Creek soils. Dr. T. W. Horst is thanked for his review of the manuscript.

REFERENCES

Bader, D. C., and C. D. Whiteman, 1989: Numerical simulation of cross-valley plume dispersion during the morning transition period. *J. Appl. Meteor.*, **28,** 652–664.

Campbell, G. S., 1985: Soil Physics With BASIC—Transport Models for Soil-Plant Systems. *Developments in Soil Science,* Vol. 14, Elsevier, 150 pp.

Deardorff, J. W., 1968: Dependence of air–sea transfer coefficients on bulk stability. *J. Geophys. Res.*, **78**(8), 2549–2556.

Doran, J. C., M. L. Wesely, W. D. Neff and R. T. McMillen, 1989: Measurements of turbulent heat and momentum fluxes in a mountain valley. *J. Appl. Meteor.*, **28,** 438–444.

Fritschen, L. J., and L. W. Gay, 1979: *Environmental Instrumentation.* Springer-Verlag, 216 pp.

——, and J. R. Simpson, 1989: Surface energy and radiation balance systems: general description and improvements. *J. Appl. Meteor.*, **28,** 680–689.

Gudiksen, P. H., and D. L. Shearer, 1989: The dispersion of atmospheric tracers in nocturnal drainage flows. *J. Appl. Meteor.*, **28,** 602–608.

Halbsguth, G. M., J. Kerschgens, H. Kraus, G. Meindl and E. Schaller, 1984: Energy fluxes in an alpine valley. *Arch. Meteor. Geophys. Bioklim.*, **33**(A), 11–20.

Hawkes, H. B., 1947: Mountain and valley winds with special reference to the diurnal mountain winds of the Great Salt Lake Region. Ph.D. Dissertation, Ohio State University, Columbus, OH, 312 pp.

Hennemuth, B., and H. Schmidt, 1985: Wind phenomena in the Dischma Valley during DISKUS. *Arch. Meteor. Geophys. Bioklim.*, **35**(B), 361–387.

Horst, T. W., K. J. Allwine and C. D. Whiteman, 1987: A thermal energy budget for nocturnal drainage flow in a simple valley. Preprints, *Fourth Conference on Mountain Meteorology,* Seattle, Amer. Meteor. Soc., 15–19.

Laulainen, N. S., C. D. Whiteman, W. E. Davis and J. M. Thorp, 1981: Mixing layer growth and background air quality measurements over the Colorado oil shale area. Preprints, *Second Conference on Mountain Meteorology,* Steamboat Springs, CO. Amer. Meteor. Soc., 165–172.

McInnes, K., 1981: Thermal conductivity of soils from dryland wheat regions in eastern Washington. M.S. Thesis, Department of Agronomy and Soils, Washington State University, Pullman, WA, 51 pp.

Miller, D. H., 1981: Energy at the Surface of the Earth. *International Geophysics Series,* Vol. 27, Academic Press, 516 pp.

Moore, R., J. Burrell and J. Nyenhuis, 1981: Soils baseline report, Clear Creek property. Rep. PA145 to Chevron Shale Oil Company, Environmental Research and Technology, Inc., Fort Collins, CO.

Ohmura, A., 1982: Objective criteria for rejecting data for Bowen ratio flux calculations. *J. Appl. Meteor.*, **21,** 595–598.

Oke, T. R., 1978: *Boundary Layer Climates.* Methuen Co. Ltd., 372 pp.

Philip, J. R., 1961: The theory of heat flux meters. *J. Geophys. Res.*, **66,** 571–579.

Post, M. J., and W. D. Neff, 1986: Doppler lidar measurements of winds in a narrow mountain valley. *Bull. Amer. Meteor. Soc.*, **67,** 274–281.

Rott, H., 1979: Vergleichende untersuchungen der energiebilanz im hochgebirge [Comparative studies of the energy balance in the high mountains]. *Arch. Meteor. Geophys. Bioklim.*, **28**(A), 211–232.

Schädler, B., 1982: The variability of evapotranspiration in the Reitholzbach Basin as determined using energy balance methods. *Mitt. Versuchsanstalt Wasserbau, Hydrologie Glaziologie,* 46E, Eidgenössische Technische Hochschule, 105 pp.

Tanner, C. B., 1967: Measurement of evaporation. *Irrigation of Agricultural Lands Agronomy Monograph* 11. R. M. Hagan, H. R. Haise and T. W. Edminster, Eds., Amer. Soc. of Agronomy, 534–574.

Whiteman, C. D., 1989: Morning transition tracer experiments in a deep narrow valley. *J. Appl. Meteor.*, **28,** 626–635.

——, and S. Barr, 1986: Atmospheric mass transport by along-valley wind systems in a deep Colorado valley. *J. Climate Appl. Meteor.*, **25,** 1205–1212.

——, K. J. Allwine, M. M. Orgill, L. J. Fritschen and J. R. Simpson, 1989: Deep valley radiation and surface energy budget microclimates. Part I: Radiation. *J. Appl. Meteor.*, **28,** 414–426.